Studies of the effect of mirror radius value on the reconstruction of the Cerenkov emission angle by MonteCarlo simulation.

P. Schiavon

COMPASS / RICH / PS / Report 4.a

14/ 5/97 - rev. 17/12/97.

1 Assumptions :

a) For the definitions of the reference systems and the geometry of the apparatus refer to the COMPASS / RICH / PS / Report 1 and 2.

b) In the simulation, particles are generated reading a GEANT pre-processed file (using the LEPTO generator), for a more realistic 'illumination' of the mirror (particle momentum > 5. GeV/c); (see COMPASS/RICH/PS/Report 1 for more details).

c) Each particle (one per event in this study), when crossing the radiator, emits Cerenkov photons, uniformely distributed in distance (s) along the path length and in angle (ϕ) around the particle trajectory; the condition $\beta = 1.$ results in a Cerenkov emission angle $\theta_C = 55.82\ mrad$ for a C4F10 (gas) radiator.

d) The whole (upper) RICH mirror is made of many (50 ?) sub-mirrors put together side by side to make a continuous spherical surface; to simplify the geometry of this simulation, the sub-mirrors have a square shape ($400.mm \times 400.mm$) instead of the exagonal shape foreseen;

e) The radii of the sub-mirrors have not the nominal value (R_0), but their values (R_g) differ to some extent from it, because of the construction procedure.

2 Procedure :

a) A sample of $\sim$ 3000 events (= particles) is typically analized; each particle is assumed to emit 30 Cerenkov photons.

b) For comparison purposes, the detector is fixed in the position of the COMPASS proposal studies, i.e. :
angle (with resp. to the vertical) = 150. $mrad$ = 8.6 deg,
position (along the z-axis, at the mirror centre level) = radiator entrance - 92. mm =

5408. mm, downstream the μ-beam target.

c) The path of each photon is simulated before and after reflection and the impact point on the detector is calculated using the actual mirror radius value (R_g);

d) Assuming measured the particle trajectory, the emission angle of each photon is then computed (see for details COMPASS/RICH/PS/Report 2);
the detector resolution is not taken into account;
in this reconstruction we use the nominal radius value (R_0) for each sub-mirror; we then compute the standard deviation (σ_θ) of the difference θ_{rec} - θ_C, where θ_C is the MC generated angle.

3 Results :

The results are presented in table 1 :

We assume that the sub-mirrors are produced with a spread in radius value around the nominal value R_0, with a distribution nearly gaussian (at least to simplify this study).

a) We assume that the radius (R_g) of each sub-mirror has a value wich is the nominal value (R_0) plus a variation which has a gaussian distribution around R_0 with a standard deviation equal to 1% of R_0 and a random distribution over the whole mirror surface; if $R_0 = 6600.\ mm$ then $\sigma_R = 66.\ mm$.
This sub-mirror configuration should then be kept fixed for all the events of the simulation run. The photons emitted by each particle are reflected towards the detector by such a sub-mirror system and σ_θ is computed.
On the other hand, the results are rather sensitive to different sub-mirror configurations, chosen with the same mechanism; it is then more reliable to take the average of σ_θ over many different configurations; this is done in practice, instead of changing the sub-mirror configuration and repeating the simulation run many times, chosing a new configuration for each event of the run.
The variation of the radius value (ΔR) alone is not enought to determine the photon optics; in fact, for a given ΔR, we can apply different alignment criteria (see fig.1):
- (a) keep the sub-mirror surface in position, moving its centre by ΔR towards the sub-mirror itself (rows 1 and 2 of table),
- (b) move the sub-mirror surface towards its centre by ΔR (row 3 of table),
- (c) move the sub-mirror centre position by ΔR along the z-axis (as common direction for all the sub-mirrors) (row 4 of table),
- (d) move the sub-mirror surface towards its centre by $\Delta R/2.$ and the sub-mirror centre position by $\Delta R/2.$ towards the sub-mirror itself (row 5 of table), and so on.
Note that using β=1. particles only, all the resolutions are worse by about 5.%.

b) A random distribution of the sub-mirrors as in point a) over the whole mirror surface is not the best solution; we can imagine to select the sub-mirrors according to the radius value and put them, e. g., in such a way that the radii grow going from inside (beam line) to outside, realizing a 'parabolic' like shape (see fig.2 (b)); (row 6 of table). The opposite situation ('anti-parabolic' shape) (see fig.2 (c)) doesn't change the quality

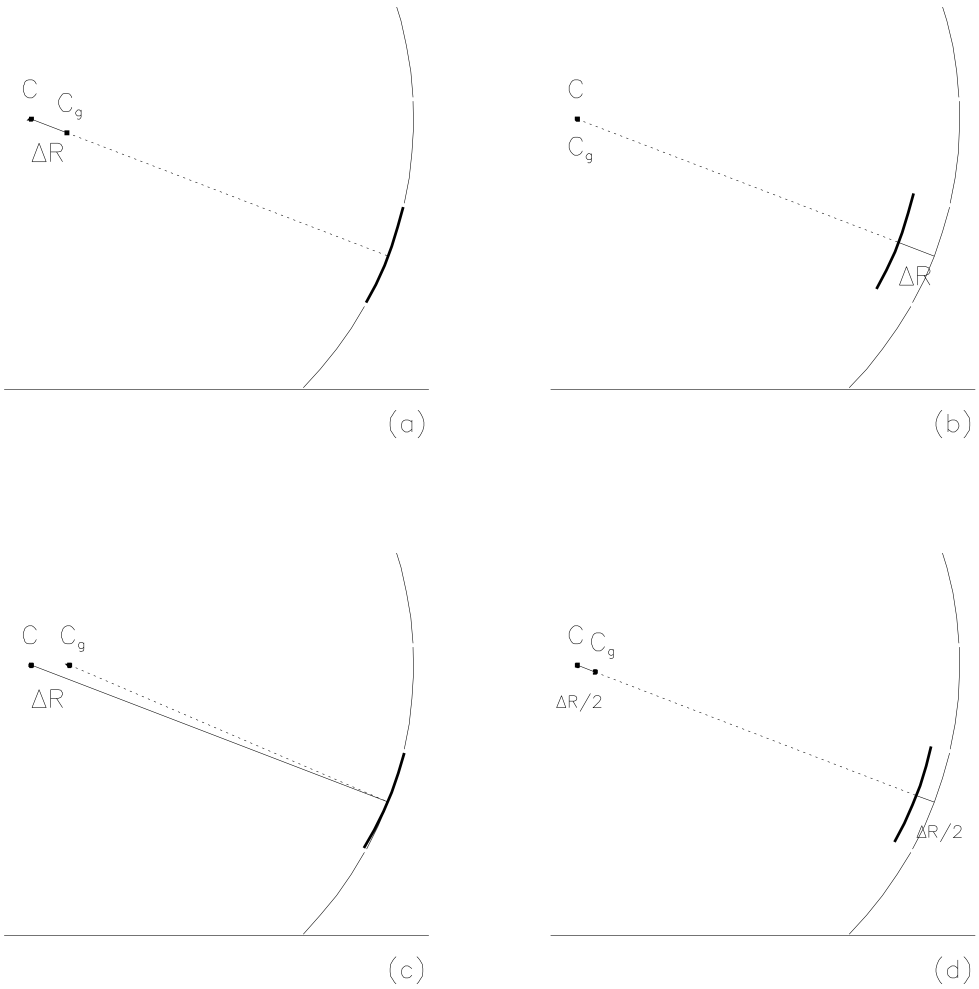

Figure 1: The figure shows four of the many different ways of interpreting the fact that a sub-mirror radius is 'wrong' by ΔR with respect to the nominal value R_0. C is the nominal centre position, C_g the actual one. In (a) the sub-mirror surface is on the whole mirror surface, but the radius is shorter of ΔR than R_0; in (b) the sub-mirror centre is fixed and its surface moved; in (c) the correction of the centre position is along the z-axis; in (d) an intermediate solution between (a) and (b) is assumed. Note that each one is a possible recipe to aligne the sub-mirrors.

of the results (row 7 of table).
Due to the particle distribution on the mirror surface (see fig.2 (d)), the sub-mirrors closest to the centre (beam line) are hit more frequently; the effective average value of ΔR is then different from 0. The results of rows 6 and 7 are obtained using in the reconstruction R_0 plus this effective average ΔR instead of R_0 itself ('corrected').

Note that the main purpose of such a choice is to put close each other the sub-mirrors whose radii differ the least (on average); given the dimensions on the mirror surface of the spot due to the photons emitted by one particle ($330.mm$ diameter for β=1.), at most four adjacent sub-mirrors will be hit for each particle (three in the real case with sub-mirror of exagonal shape) and, knowing the values of the radii and the particle impact point on the mirror, an average value over 4 (or 3) sub-mirrors can be used instead; note that this correction is not yet applied to the procedure.

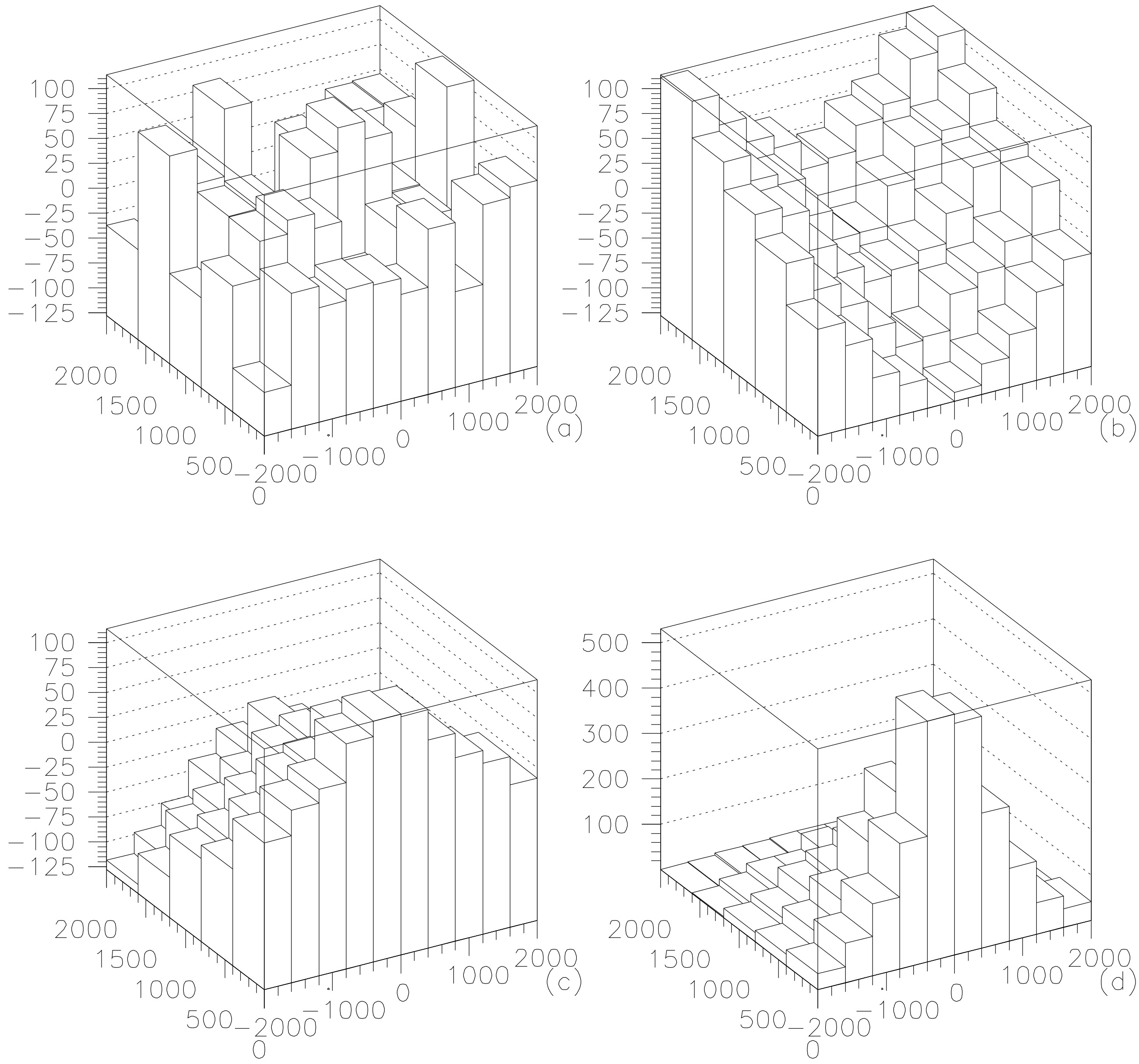

Figure 2: The figure shows: (a) a random distribution of ΔR; (b) the same ΔR sample arranged in a 'parabolic' or (c) in an 'anti-parabolic' distribution; the horizontal plane of the plots shows the x- and y-position of the sub-mirrors (the beam line is at 0., 0.), the vertical axis, ΔR. In (d) the particle distribution on the sub-mirrors is shown instead.

c) For a crude comparison, let's assume that the whole mirror has a radius value of 0.5% (33. mm) less than R_0, but it is in the correct position (recipe (a)); the resulting resolution is shown in row 8 of the table.

4 Comments :

a) Varying radius and centre towards the sub-mirror by ΔR, we keep the mirror surface in place and the result is clearly better; varying the radius only of the various

row	mirror configuration	σ_R	alignment mode	σ_θ μrad
1	fixed averaged	1. %	(a)	184.
2	fixed averaged	0.5 %	(a)	92.
3	fixed averaged	1. %	(b)	470.
4	fixed averaged	1. %	(c)	202.
5	fixed averaged	1. %	(d)	430.
6	'parabolic' corrected	1. %	(a)	171.
7	'anti-parab.' corrected	1. %	(a)	163.
8	fixed whole mirror	0.5 %	(a)	202.
9	spherical aberr. only			95.
10	pixel only			156.

Table 1: Resolution σ_θ in reconstructed Cerenkov angle θ_C (RICH 1). In rows 1 to 5 is shown the resolution due to a distribution in ΔR, the difference between the actual value (R_g) and the nominal one (R_0) of each mirror element (sub-mirror), taking into account different ways ((a) to (d)) of sub-mirror positioning; see text and fig.1 for more details. In rows 6 and 7 specific sub-mirror arrangements ('parabolic' and 'anti-parabolic' like shapes) are assumed; row 8 is for comparison. In row 9 the order of magnitude of the contribution to the total resolution due to the spherical aberrations only and and in row 10 of the experimental resolution only ($8.mm \times 8.mm$ pixels) (to be added in quadrature).

sub-mirrors, we create a discontinuous surface for the whole mirror with quite a worse result.

b) No appreciable difference between 'parabolic' and 'anti-parabolic' shape, after correction.

c) An improvement on the average resolution can be expected on the basis of the following argument: we assume that the whole sample of sub-mirrors is produced with some spread in radius, e.g., 1.%; only one half of the sub-mirrors will make the upper mirror surface of RICH1, the second half the lower one; we can then divide in two the sample, taking e.g. larger radius sub-mirrors for the upper part and smaller for the lower, with different average (nominal) values from upper to lower, but smaller (factor of 2?) spread in value.